INTERNATIONAL JOURNAL OF REFRIGERATION 34 (2011) 1649–1656

available at www.sciencedirect.com

journal homepage: www.elsevier.com/locate/ijrefrig

Design-theoretical study of cascade CO_2 sub-critical mechanical compression/butane ejector cooling cycle

V.O. Petrenko[a,b,*], B.J. Huang[a], V.O. Ierin[b]

[a] New Energy Center, Department of Mechanical Engineering, National Taiwan University, Taipei 106, Taiwan
[b] Odessa State Academy of Refrigeration, Ejector Refrigeration Technology Center, 1/3, Dvoryanskaya St., 65082 Odessa, Ukraine

ARTICLE INFO

Article history:
Received 17 February 2010
Received in revised form
3 November 2010
Accepted 27 November 2010
Available online 3 December 2010

Keywords:
Carbon dioxide
Butane
Cascade system
Vapor
Compression
Ejector

ABSTRACT

In this paper an innovative micro-trigeneration system composed of a cogeneration system and a cascade refrigeration cycle is proposed. The cogeneration system is a combined heat and power system for electricity generation and heat production. The cascade refrigeration cycle is the combination of a CO_2 mechanical compression refrigerating machine (MCRM), powered by generated electricity, and an ejector cooling machine (ECM), driven by waste heat and using refrigerant R600. Effect of the cycle operating conditions on ejector and ejector cycle performances is studied. Optimal geometry of the ejector and performance characteristics of ECM are determined at wide range of the operating conditions. The paper also describes a theoretical analysis of the CO_2 sub-critical cycle and shows the effect of the MCRM evaporating temperature on the cascade system performance. The obtained data provide necessary information to design a small-scale cascade system with cooling capacity of 10 kW for application in micro-trigeneration systems.

Etude sur la conception et sur un cycle théorique de refroidissement à compression mécanique en cascade au CO_2 subcritique, muni d'un système à éjecteur au butane

Mots clés : Dioxyde de carbone ; Butane ; Système à cascade ; Vapeur ; Compression ; Éjecteur

1. Introduction

Trigeneration or combined heating, cooling and power (CHCP) production is becoming an increasingly important energy-saving option, particularly on a small-scale basis. Conventional CHCP system is the combination of a traditional combined heat and power (CHP) system that cogenerates electricity and heat, with an absorption cycle, which is driven by waste heat.

Different types of trigeneration systems can be designed using reliable ejector cooling machines (ECMs) operating with low-boiling point working fluids and powered by waste heat

* *Corresponding author*. New Energy Center, Department of Mechanical Engineering, National Taiwan University, Taipei 106, Taiwan. Tel.: +88 62 33662686; fax: +88 62 23671182.
E-mail addresses: volya@paco.net, volyablacksea@yandex.ru (V.O. Petrenko).
0140-7007/$ – see front matter
doi:10.1016/j.ijrefrig.2010.11.012

Nomenclature

A	area (mm^2)
C	ejector compression ratio
c_p	constant pressure specific heat (kJ kg^{-1} K^{-1})
CHP	combined heat and power
CHCP	combined heating, cooling and power
COP	coefficient of performance
E	ejector expansion ratio
ECM	ejector cooling machine
GWP	Global Warming Potential
h	specific enthalpy (kJ kg^{-1})
ICE	internal combustion engine
l	specific compressor work (kJ kg^{-1})
$\dot{m}$	mass flow rate (kg s^{-1})
MCRM	mechanical compression refrigerating machine
P	pressure (bar)
Q	heat flow (kW)
q	specific heat of evaporation (kJ kg^{-1})
r	compressor pressure ratio
s	specific entropy (kJ kg^{-1} K^{-1})
T	temperature (°C or K)
v	specific volume (m^3 kg^{-1})
$\dot{W}$	power (kW)
$\dot{w}$	specific power consumption (kW kW^{-1})

Greek letters

α, β	ejector area ratios
γ	converging angle at mixing chamber entrance
Δ	difference
η	coefficient of efficiency
ω	entrainment ratio

Subscripts

b	boiling
BC	bottoming cycle
c	condenser
C	compressor
CB	condenser bottoming
crit	critial
cs	compressor isentropic
e	evaporator
eg	electric generator
ET	evaporator topping
g	generator
m	motor
mech	mechanical
opt	optimum
p	primary
pump	feed pump
s	secondary
sup	superheating
t	throat
therm	thermal
2, 3	cross-sections of the ejector (Fig. 3, Equations (2) and (3))
1, 2, 3…13	cycle states in the Figs. 1 and 2, Equations (5)–(20)
2s	location downstream of the isentropic process

supplied from CHP systems. Recently several high-efficiency ECMs operating with refrigerants R141b and R245fa were developed and coefficients of performance (COPs) in the range of 0.5–0.7 were obtained experimentally at practical operating conditions (Huang et al., 1999; Eames et al., 2007).

Hydrofluorocarbon refrigerants, which have been developed as alternatives to chlorofluorocarbon and hydrochlorofluorocarbon refrigerants, are known to have a high Global Warming Potential (GWP). As a result of this environmentally benign, natural refrigerants have attracted considerable recent attention. The natural refrigerants include ammonia, hydrocarbons, carbon dioxide, water, air, etc. These natural refrigerants have zero Ozone Depleting Potential and the majority of them have negligible GWP.

A distinctive feature of the proposed micro-trigeneration system is that it combines a conventional CHP system and a cascade CO_2 sub-critical mechanical compression/heat-driven ejector cooling cycle using a natural low-boiling working fluid.

Carbon dioxide (CO_2) is a good refrigerant. The key advantages of CO_2 include the fact that it is easily available, environmental friendly, non-toxic, and not explosive. CO_2 has relatively high working pressures, which give small vapor volume that leads to compact components. Thermo-physical properties of carbon dioxide are excellent. Heat transfer coefficients are high and sensitivity to pressure drop is low. Since the critical temperature of CO_2 is rather low (31.1 °C), sub-critical operation is only possible when the average heat sink temperature is rather low. In the event that sub-critical operation is feasible it may be stated that the CO_2 systems compete very well in energy efficiency with systems using other refrigerants. Additionally, CO_2 cycle performance and reliability can be significantly increased by reducing the discharge pressure. This requires operation in the sub-critical mode (Robinson and Groll, 1998; Neksa et al., 2001; Chen and Gu, 2005; Lee et al., 2006).

This research aims to carry out a theoretical study for the design of a small-scale cascade refrigeration cycle utilizing a CO_2 sub-critical mechanical compression cycle and low-grade waste heat-driven ejector cooling cycle operating with low-boiling environmentally friendly working fluid. The waste-heat driven ECM is used to cool the condenser of MCRM to reduce its condensing temperature to increase the performance.

The analysis and comparison of performance characteristics for various low-boiling point refrigerants had shown that from the thermodynamic and operating viewpoints the most suitable for ECMs are low-pressure refrigerants which have high critical temperature T_{crit}, large specific latent heat at evaporating temperature T_e, small specific heat of liquid refrigerant in the range of operating temperatures (T_g–T_e), and normal boiling temperature $T_b \leq T_e$. The calculations show that environmentally friendly working fluid R600 has higher performances than other refrigerants (Petrenko, 2001; Petrenko et al., 2005a).

Consequently refrigerant R600 (butane) is selected as the working fluid for low-grade waste heat-driven ECM in the present study.

2. Design of micro-trigeneration system

A diagram of the proposed micro-trigeneration system incorporating a CHP system and a cascade refrigeration cycle is shown in Fig. 1.

In CHP systems two kinds of prime movers are generally used: reciprocating internal combustion engines (ICEs) and gas micro-turbines which both can be selected to exactly match the site conditions.

From Fig. 1, the CHP system consists of ICE, electric generator producing electric power $\dot{W}_{eg}$ and heat recovery unit. The cascade refrigeration cycle is the combination of a CO_2 sub-critical mechanical compression refrigerating machine (MCRM), powered by generated electricity, and an ECM driven by waste heat. Thus, the significant part of the exhaust heat can be recovered. Such waste heat recovery would ultimately reduce overall fuel consumption and CO_2 emission and thus helps to alleviate global climatic change brought about by the greenhouse effect (Petrenko et al., 2005b).

The ECM acts as the topping cycle and the MCRM acts as the bottoming cycle in the cascade system. The two cycles are thermally connected through the cascade condenser, which serves as evaporator for the topping cycle and the condenser of the bottoming cycle.

The low-temperature (bottoming) cycle with CO_2 as working fluid can be used for refrigeration at temperature levels found suitable in supermarkets, cold stores or food processing plants. The high-temperature (topping) cycle operating with butane as refrigerant is used to condense the CO_2 vapor of the low-temperature cycle in cascade condenser.

Fig. 2 shows the thermodynamic processes of the CO_2 and R600 cycles in *lgP-h* diagram. The operating principle of cascade refrigeration cycle is as follows. In the MCRM the compressed carbon dioxide coming from the compressor is

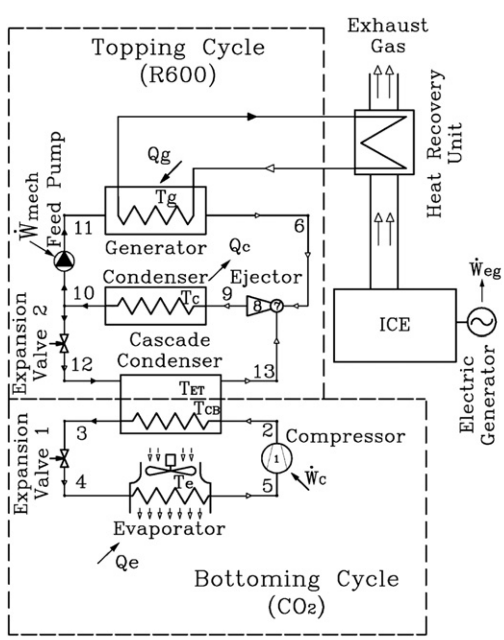

Fig. 1 – Diagram of micro-trigeneration system incorporating a CHP system and a cascade refrigeration cycle.

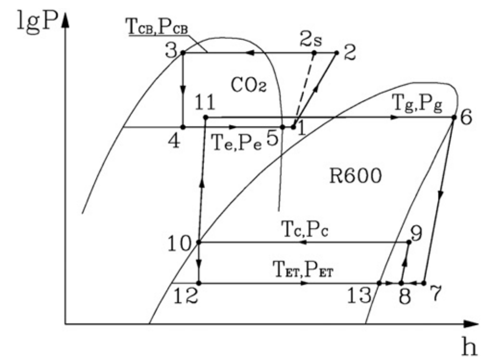

Fig. 2 – Cascade CO_2 sub-critical mechanical compression/R600 ejector cooling cycle in *lgP-h* diagram.

condensed in the cascade condenser at a condensing temperature T_{CB}. The liquid refrigerant then expands through an expansion valve 1 and enters the evaporator where it is evaporated at low evaporating temperature T_e to produce the necessary cooling effect Q_e for refrigeration purposes. After the evaporator the entrained vapor is compressed to a high pressure state by the compressor, before entering the cascade condenser. This completes the CO_2 sub-critical mechanical compression refrigeration cycle.

Low-grade heat Q_g is delivered from the heat recovery unit to the generator of ECM, where liquid refrigerant is vaporized at relatively high generating pressure P_g and temperature T_g. This primary vapor with a mass flow rate of $\dot{m}_p$ flows through the primary convergent-divergent nozzle of the ejector and accelerates within it. At the exit of the nozzle, the accelerated flow becomes supersonic, and induces a locally low pressure region. The relatively low pressure produced by this expansion causes a suctioning effect of secondary flow with a mass flow rate of $\dot{m}_s$ from the cascade condenser at low pressure P_{ET}. The primary and secondary fluids are mixed in the mixing section of the ejector and undergo a pressure recovery process in the diffuser section. The combined stream flows to the condenser where it is condensed to liquid at intermediate condensing pressure P_c and temperature T_c. The heat of condensation Q_c is rejected to the environment. Then, the condensate is divided into two parts, one is pumped back to the generator, and the other is expanded through an expansion valve 2 to a low-pressure state and enters the cascade condenser, where it is evaporated at low pressure P_{ET} and temperature T_{ET} by the condensation heat from the MCRM. The vapor is finally entrained by the ejector, thus completing the exhaust heat-driven ejector cooling cycle. The resulting cooling effect Q_{ET} is used to provide rejection of condensation heat from cascade condenser.

3. Analysis of ejector design and ejector cooling cycle performance

The supersonic ejector is the key component in the ejector cooling cycle. It is a simple jet device which is used in the ejector cycle for suction, compression, and discharge of the secondary vapor by force of the primary vapor.

Fig. 3 illustrates the structure of supersonic ejectors with cylindrical (a) and conical–cylindrical (b) mixing chambers. The ejector assembly can be divided into four main parts: a nozzle, a suction chamber, a mixing chamber, and a diffuser.

Operating conditions of the ejector are specified by operating pressures P_{ET}, P_c, P_g, expansion pressure ratio $E = P_g/P_{ET}$ and compression pressure ratio $C = P_c/P_{ET}$.

The performance of the ejector is measured by its entrainment ratio ω which is the ratio between the secondary and the primary fluid mass flow rates $\dot{m}_s$ and $\dot{m}_p$, as shown in the following equation:

$$\omega = \frac{\dot{m}_s}{\dot{m}_p} \quad (1)$$

The design of the ejector flow profile with a cylindrical mixing chamber is determined by the area ratio α which is defined as the cross-section area of the cylindrical mixing section A_3 divided by that of the primary nozzle throat area A_t, which can be found from Eq. (2):

$$\alpha = \frac{A_3}{A_t} \quad (2)$$

The design of a conical–cylindrical mixing chamber is specified by area ratio α, converging angle γ at mixing chamber entrance, and the area ratio β, which is defined as the entrance area A_2 of the conical part of mixing chamber divided by that of the cross-section area A_3, as shown in Eq. (3):

$$\beta = \frac{A_2}{A_3} \quad (3)$$

Construction, geometry and surface condition of supersonic ejector flow profile must provide the most effective utilization of primary flow energy for suction, compression, and discharge of the secondary vapor (Petrenko, 1978; Huang et al., 1999; Eames et al., 2004, 2007; Petrenko et al., 2005a, 2005b).

On the basis on the improved 1-D model of ejector, design area ratio α and the optimum value of β can be found with application of variational calculation (Huang et al., 1999). The value of β_{opt} corresponds to the maximum of entrainment ratio ω. Supplementary data for the determination of the α, β_{opt} and optimal converging angle γ are given in Petrenko (1978) and Petrenko et al. (2005a).

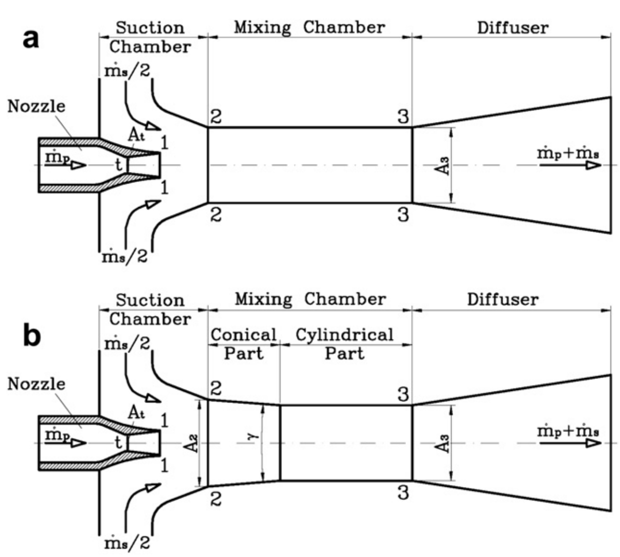

Fig. 3 – Structure of supersonic ejectors with cylindrical (a) and conical–cylindrical (b) mixing chambers.

Theoretical and experimental investigations of supersonic ejectors with conical–cylindrical and cylindrical mixing chambers operating with various refrigerants demonstrate convincingly that the application of conical–cylindrical mixing chambers at the same operating conditions causes an improvement up to 25–35% in ω compared with cylindrical mixing chambers. The primary cause of this improvement is decreasing of the irreversibilities of gas-dynamic processes, which occur in the mixing chamber of the supersonic ejector. The advantage of ejectors with optimal design of conical–cylindrical mixing chambers is especially revealed at high critical condensing temperatures T_c (Petrenko, 1978; Petrenko et al., 2005a, 2005b).

The performance of the ECM is usually measured by a single COP, which is the ratio of the useful cooling effect produced in the evaporator over the gross energy input into the ejector cycle required to produce the cooling effect. But it should be taken into account that the ECM commonly utilizes a mechanical feed pump, and, consequently, an input of some amount of mechanical power $\dot{W}_{mech}$ in addition to a low-grade thermal energy Q_g.

However, in spite of the fact that the mechanical power $\dot{W}_{mech}$, consumed by the feed pump is very small compared to the thermal energy Q_g input to the generator to actuate ejector, it may not be omitted (Petrenko, 2001).

Therefore, from both thermodynamic and economic points of view, the efficiency of the topping ECM cycle can be correctly characterized by using separately both thermal COP_{therm} and actual specific power consumption of mechanical feed pump $\dot{w}_{mech}$. The value of COP_{therm} is defined as the cooling load at the cascade condenser Q_{ET} divided by the thermal energy Q_g, and the value of $\dot{w}_{mech}$ is the ratio between the mechanical power $\dot{W}_{mech}$ and the cooling effect Q_{ET}. They can be expressed as Eqs. (4) and (5):

$$COP_{therm} = \frac{Q_{ET}}{Q_g} = \frac{\dot{m}_s q_{ET}}{\dot{m}_p q_g} = \omega \frac{q_{ET}}{q_g} \quad (4)$$

$$\dot{w}_{mech} = \frac{\dot{W}_{mech}}{Q_{ET}} = \frac{\dot{m}_p \upsilon_5 (P_g - P_c)}{\eta_{pump} \dot{m}_s q_{ET}} = \frac{\upsilon_5 (P_g - P_c)}{\eta_{pump} \omega\, q_{ET}} \quad (5)$$

where υ_5 and η_{pump} are specific volume of intake refrigerant and feed pump coefficient of efficiency, respectively; $(P_g - P_c)$ is the generating and condensing pressure difference, kPa.

It should be observed that the electrically driven feed pump is the only component in the ejector cycle which has moving parts and therefore determines the reliability, leakproofness, and lifetime of the whole system. Instead of using the conventional electrically driven feed pumps for ECMs operating with flammable refrigerants such as butane, utilization of hermetic float-type thermo-gravity feeders which are designed for application in various small capacity ejector systems is very attractive (Petrenko et al., 2005b).

From the steady energy balance for the ECM using the numbering in Figs. 1 and 2, the cooling load at the cascade condenser Q_{ET}, the heat load at the generator Q_g, the heat load at the condenser Q_c and the actual power consumption of mechanical feed pump $\dot{W}_{mech}$ can be expressed as Eqs. (6)–(9):

$$Q_{ET} = Q_{CB} = (h_{13} - h_{12})\dot{m}_s \quad (6)$$

$$Q_g = (h_6 - h_{11})\dot{m}_p \quad (7)$$

$$Q_c = Q_{ET} + Q_g = (h_9 - h_{10})(\dot{m}_s + \dot{m}_p) \quad (8)$$

$$\dot{W}_{mech} = \frac{\dot{m}_p v_5 (P_g - P_c)}{\eta_{pump}} \quad (9)$$

where h_{13} and h_{12}, h_6 and h_{11}, h_{10} and h_9 are the outlet and inlet refrigerant enthalpies at the cascade condenser, at the generator and at the condenser, respectively.

4. Analysis of CO_2 sub-critical compression refrigeration cycle

Analysis of CO_2 sub-critical mechanical compression refrigeration cycle is described as follows. From the steady energy balance for the MCRM and using the numbering in Figs. 1 and 2, a specific cooling capacity q_e, a specific condensing heat q_{CB} and a specific isentropic compressor work l_{cs} may be computed by Eqs. (10)–(12):

$$q_e = h_5 - h_4 \quad (10)$$

$$q_{CB} = h_2 - h_3 \quad (11)$$

$$l_{cs} = h_{2s} - h_1 \quad (12)$$

where h_5 and h_4, h_3 and h_2, h_{2s} and h_1 are the outlet and inlet refrigerant enthalpies at the evaporator, at the cascade condenser and at the compressor, respectively.

Actual specific work of the compressor is defined as follows:

$$l_C = h_2 - h_1 = (h_{2s} - h_1)/\eta_{cs} \quad (13)$$

where η_{cs} is the isentropic efficiency of the compressor.

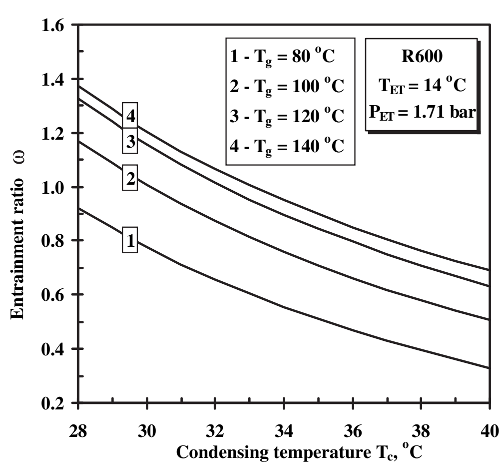

Fig. 4 – Variation of ω with T_c at different T_g for T_{ET} = 14 °C.

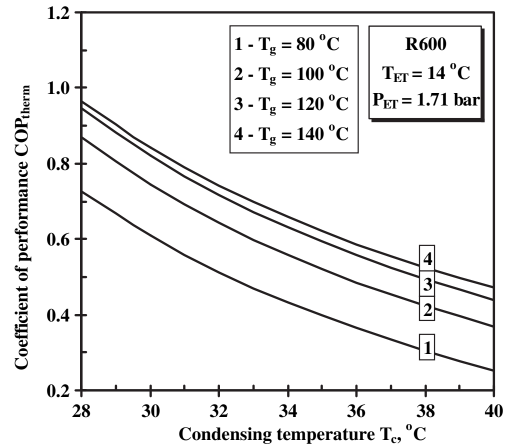

Fig. 5 – Variation of COP_{therm} with T_c at different T_g for T_{ET} = 14 °C.

And the enthalpy of the outlet of the compressor can be expressed as Eq. (14):

$$h_2 = h_1 + \frac{h_{2s} - h_1}{\eta_{cs}} \quad (14)$$

For the chosen semi-hermetic CO_2 type compressor η_{cs} can be written as the function of the ratio of compressor discharge and suction pressures $r = P_{CB}/P_e$. The correlation obtained by best fitting the experimental data for CO_2 sub-critical refrigeration cycle (Neksa et al., 2001; Lee et al., 2006) has the following form:

$$\eta_{cs} = 0.8981 - 0.09238\, r + 0.00476\, r^2 \quad (15)$$

The CO_2 cycle coefficient of performance is defined as the specific cooling effect at the evaporator q_e, divided by the actual specific compressor work l_C, as shown in Eq. (16):

$$COP_{BC} = \frac{q_e}{l_C} = \frac{h_5 - h_4}{h_2 - h_1} \quad (16)$$

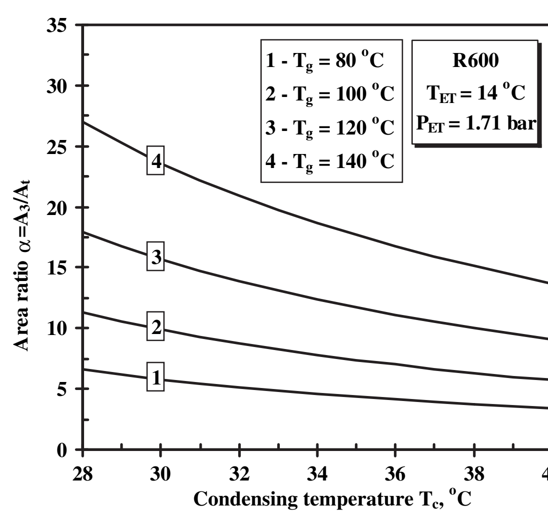

Fig. 6 – Variation of $\alpha = A_3/A_t$ with T_c at different T_g for T_{ET} = 14 °C.

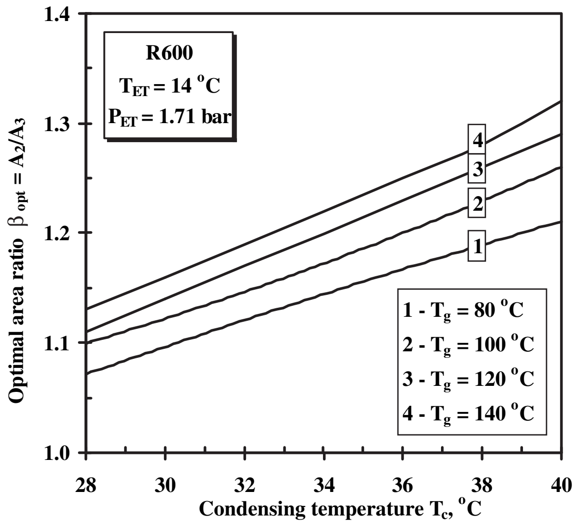

Fig. 7 – Variation of optimal area ratio $\beta_{opt} = A_2/A_3$ with T_c at different T_g for $T_{ET} = 14\ ^\circ C$.

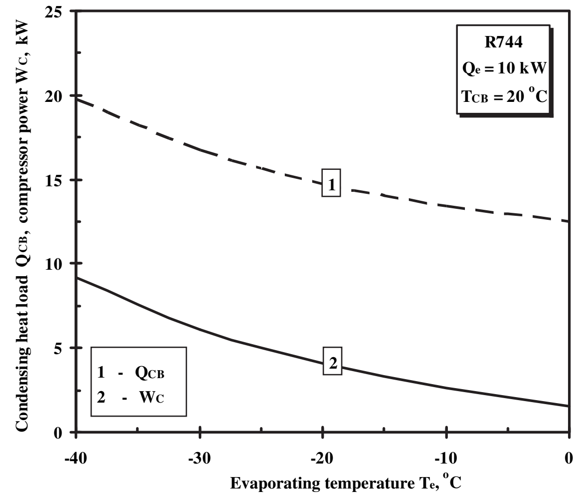

Fig. 9 – Variation of Q_{CB} and $\dot{W}_C$ with T_e for $Q_e = 10$ kW at $T_{CB} = 20\ ^\circ C$.

The values of the refrigeration output of the compression cycle Q_e, the compressor power consumption $\dot{W}_C$, and the heat load at the cascade condenser Q_{CB} are found respectively from Eqs. (17)–(19):

$$Q_e = q_e \dot{m} \tag{17}$$

$$\dot{W}_C = l_C \dot{m} \tag{18}$$

$$Q_{CB} = q_{CB} \dot{m} \tag{19}$$

where $\dot{m}$ is the mass flow rate of carbon dioxide in the bottoming cycle.

Internal superheating caused by the semi-hermetic compressor motor can be calculated from Eq. (20):

$$\Delta T_{sup} = T_1 - T_5 = \frac{1}{c_p}(h_2 - h_1)\left(\frac{1}{\eta_m} - 1\right) \tag{20}$$

where c_p is constant pressure specific heat of carbon dioxide, η_m is the coefficient of efficiency of the motor.

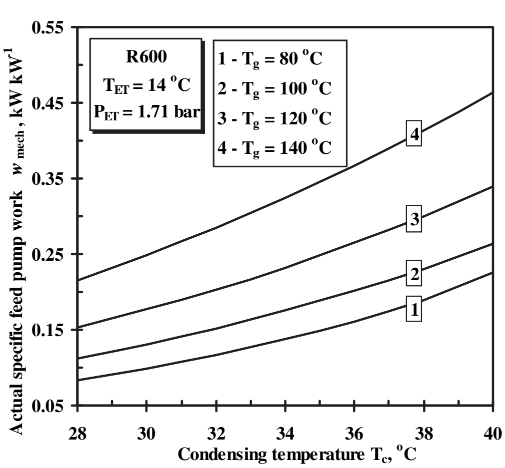

Fig. 8 – Variation of $\dot{w}_{mech}$ with T_c at different T_g for $T_{ET} = 14\ ^\circ C$ and $\eta_{pump} = 0.5$.

All the calculations were performed using the REFPROP 8.0 (Lemmon et al., 2007).

5. Results and discussions

In order to predict the ejector and ECM performance, a computer simulation program based on the improved 1-D model of the ejector has been used. This program calculates the performance of the ejector and ECM at critical-mode operating conditions and provides optimum design data for the ejector system (Huang et al., 1999; Petrenko et al., 2005a). The model validation against the refrigerants R141b, R236fa and R245fa experimental data has shown very good agreement under the wide ranges of design and off-design operating conditions (Huang et al., 1999; Eames et al., 2004, 2007).

The program has been used for the theoretical study of the topping ejector cycle and supersonic ejector with conical–cylindrical mixing chambers, operating with butane. For the present study the ejector and the ECM were investigated

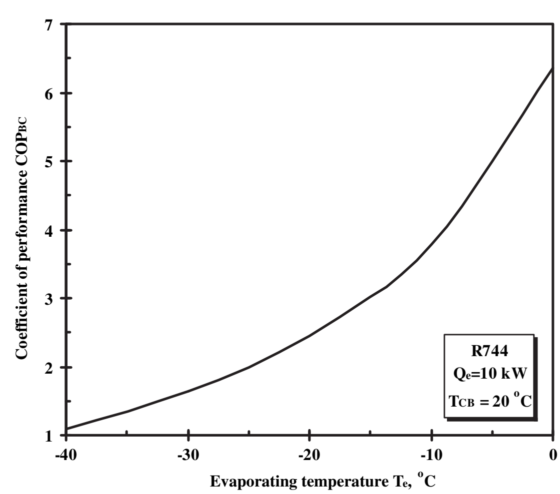

Fig. 10 – Variation of COP_{BC} with T_e for $Q_e = 10$ kW at $T_{CB} = 20\ ^\circ C$.

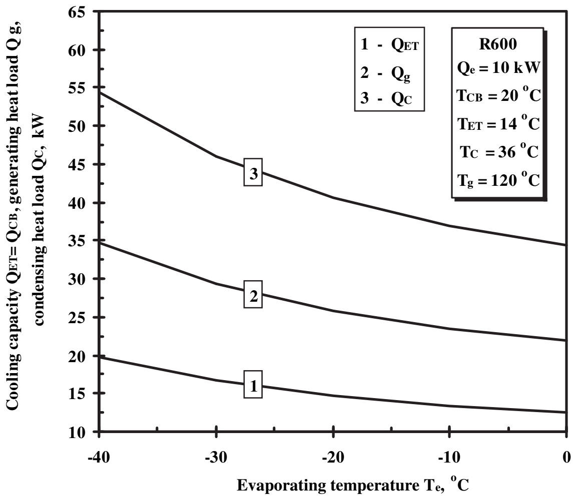

Fig. 11 – Variation of Q_{ET}, Q_c and Q_g with T_e for Q_e = 10 kW at T_{CB} = 20 °C, T_{ET} = 14 °C, T_c = 36 °C, T_g = 120 °C.

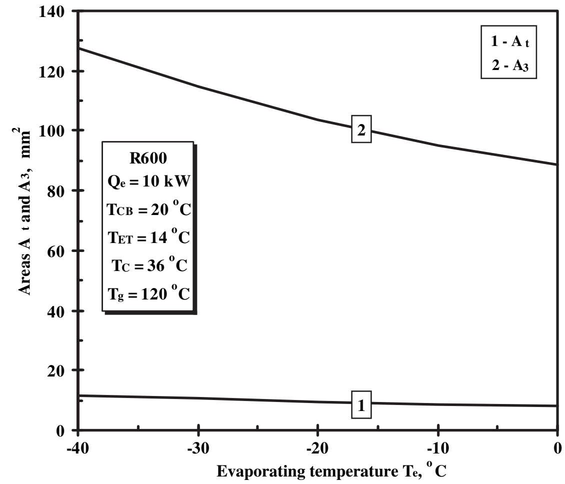

Fig. 13 – Variation of A_t and A_3 with T_e for Q_e = 10 kW at T_{CB} = 20 °C, T_{ET} = 14 °C, T_c = 36 °C, T_g = 120 °C.

over wide ranges of critical condensing temperatures T_c = 28–40 °C, and generating temperatures T_g of 80, 100, 120, 140 °C at the fixed evaporating temperature T_{ET} = 14 °C for application in the topping cycle of the cascade system.

The results of the theoretical study presented in Figs. 4–13 are obtained for design critical-mode operating conditions. Figs. 4–8 illustrate the variations of ω, COP_{therm}, A_3/A_t, A_2/A_3 and $\dot{w}_{mech}$ with T_c at different T_g for T_e = 14 °C and ejectors with optimal value of $\beta_{opt} = A_2/A_3$. Referring to Figs. 4–6 the characteristics of ω, COP_{therm}, and A_3/A_t have the same trend, and they increase with decreasing T_c and increasing T_g. It can be seen from Fig. 7 that β_{opt} increases with increasing of T_c and T_g. Fig. 8 shows that actual specific power consumption of mechanical feed pump $\dot{w}_{mech}$ decreases with decreasing T_c and T_g.

The CO_2 sub-critical cycle at the presented stage of the design-theoretical study has been investigated with fixed cooling capacity Q_e = 10 kW and fixed condensing temperature T_{CB} = 20 °C with specified temperature difference $\Delta T = T_{CB} - T_{ET}$ = 6 °C in the CO_2/R600 cascade condenser. The evaporating temperatures T_e used in the parametric study are taken in the range from −40 °C to 0 °C with assumed internal superheating in semi-hermetic compressor ΔT_{sup} of 10 °C.

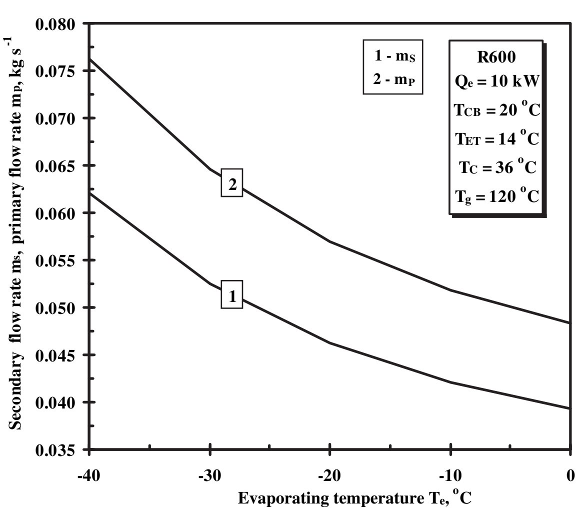

Fig. 12 – Variation of $\dot{m}_s$ and $\dot{m}_p$ with T_e for Q_e = 10 kW at T_{CB} = 20 °C, T_{ET} = 14 °C, T_c = 36 °C, T_g = 120 °C.

Table 1 – Design performance specification of CO_2 – R600 cascade cooling machine.

Parameter	Value
Bottoming cycle (R744)	
Cooling capacity, Q_e	10 kW
Evaporating temperature, T_e	−20 °C
Evaporating pressure, P_e	19.7 bar
Compressor power input, $\dot{W}_C$	4.07 kW
Superheating capacity in motor, Q_{sup}	0.68 kW
Condensing heat load, Q_{CB}	14.75 kW
Condensing temperature, T_{CB}	20 °C
Condensing pressure, P_{CB}	57.3 bar
Compressor type	semi-hermetic
Compressor isentropic efficiency, η_{cs}	0.67
Design $COP_{BC} = Q_e/\dot{W}_C$	2.46
Topping cycle (R600)	
Cooling capacity, $Q_{ET} = Q_{CB}$	14.75 kW
Evaporating temperature, T_{ET}	14 °C
Evaporating pressure, P_{ET}	1.71 bar
Condensing heat load, Q_c	40.65 kW
Condensing temperature, T_c	36 °C
Condensing pressure, P_c	3.4 bar
Generating heat load, Q_g	29.5 kW
Generating temperature, T_g	120 °C
Generating pressure, P_g	22.1 bar
Entrainment ratio, $\omega = \dot{m}_s/\dot{m}_p$	0.81
Design $COP_{therm} = Q_{ET}/Q_g$	0.57
Pressure difference, P_g–P_c	18.7 bar
Actual power consumption of feed pump, $\dot{W}_{mech}$	0.38 kW
Actual specific power consumption of feed pump, $\dot{w}_{mech}$	0.026 kW kW^{-1}
Feed pump coefficient of efficiency, η_{pump}	0.5
Design area ratio $\alpha = A_3/A_t$	10.9
Design optimal area ratio $\beta_{opt} = A_2/A_3$	1.19

Fig. 9 shows the variations of Q_{CB} and $\dot{W}_C$ with T_e of MCRM for $Q_e = 10$ kW at $T_{CB} = 20$ °C. As seen in Fig. 9 both of Q_{CB} and $\dot{W}_C$ are decreasing with increasing T_e.

Fig. 10 illustrates the variations of COP_{BC} with T_e for $Q_e = 10$ kW at $T_{CB} = 20$ °C. The results shown in this figure illustrate that increase in T_e results in a rising in the COP_{BC} of bottoming cycle. It is obvious that the COP_{BC} increases from 1.3 to 6.4 when the T_e varies from −40 °C to 0 °C.

Figs. 11–13 show the influence of the evaporating temperature T_e on the heat loads Q_{ET}, Q_g, Q_c, mass flow rates $\dot{m}_s$ and $\dot{m}_p$ of the ECM cycle, areas A_t and A_3 of ejector with β_{opt} for $Q_e = 10$ kW at $T_{CB} = 20$ °C, $T_{ET} = 14$ °C, $T_c = 36$ °C, $T_g = 120$ °C.

From Figs. 11–13 it is seen that T_e not only affects the bottoming MCRM CO_2 cycle but also the topping ECM cycle operating with butane.

Referring to Figs. 11 and 12 the heat loads Q_{ET}, Q_g, Q_c and mass flow rates $\dot{m}_s$ and $\dot{m}_p$ have the same trend, notably they are decreasing with the increasing in T_e.

Fig. 13 shows that A_t reduces very slowly almost linearly with increasing T_e, while A_3 falls more rapidly.

On the basis of the obtained results a pilot cascade CO_2 sub-critical mechanical compression/butane ejector refrigerating unit with design performance characteristics listed in Table 1 is developed. This small-scale refrigerating unit is designed for application in micro-trigeneration systems incorporating reciprocating internal combustion engines and gas micro-turbines.

6. Conclusions

In this paper an innovative micro-trigeneration system, composed of a cogeneration system and a cascade refrigeration cycle, is proposed. The cogeneration system is a combined heat and power system for electricity generation and heat production. The cascade refrigeration cycle is the combination of a mechanical compression refrigerating machine, operating with CO_2, and an ejector cooling machine, driven by waste heat and using butane as the working fluid.

According to theoretical study for the design of small-scale cascade CO_2 − R600 refrigerating unit powered by CHP system, the most important findings are as follows.

(1) Effect of the cascade cycle operating conditions on ECM and MCRM cycles performance characteristics is studied and optimal geometry of the ejector is determined. It is defined that for $Q_e = 10$ kW at $T_{CB} = 20$ °C, increase in T_e results in a rising in the COP_{BC} of bottoming cycle. COP_{BC} increases from 1.3 to 6.4 when the T_e varies from −40 °C to 0 °C.
(2) The obtained data provide necessary information to design a pilot small-scale CO_2 − R600 cascade refrigerating unit with cooling capacity of 10 kW for application in micro-trigeneration systems.
(3) The proposed micro-trigeneration system is environmentally friendly, energy-saving and potentially high performance and cost-beneficial installation that consolidates the advantages of both ECM and MCRM cycles.

Acknowledgements

This publication is based on the work supported by Award No. KUK-C1-014-12, made by King Abdullah University of Science and Technology (KAUST), Saudi Arabia.

REFERENCES

Chen, Y., Gu, J., 2005. The optimum high pressure for CO_2 transcritical refrigerating systems with internal heat exchangers. Int. J. Refrigeration 28 (8), 1238–1249.
Eames, I.W., Ablwaifa, A.E., Petrenko, V.O., 2007. Results of an experimental study of an advanced jet-pump refrigerator operating with R245fa. Appl. Therm. Eng. 27, 2833–2840.
Eames, I.W., Petrenko, V.O., Ablwaifa, A.E., 2004. Design and experimental investigation of a jet pump refrigerator. In: Proc. 3rd International Conference on Heat Powered Cycles – HPC Larnaca, Cyprus.
Huang, B.J., Chang, J.M., Wang, C.P., Petrenko, V.O., 1999. A 1-D analysis of ejector performance. Int. J. Refrigeration 22 (5), 354–364.
Lee, T.S., Liu, C.H., Chen, T.W., 2006. Thermodynamic analysis of optimal condensing temperature of cascade-condenser in CO_2/NH_3 cascade refrigeration systems. Int. J. Refrigeration 29, 1100–1108.
Lemmon, E.W., Huber, M.L., McLinden, M.O., 2007. NIST Standard Reference Database 23: Reference Fluid Thermodynamic and Transport Properties-REFPROP, Version 8.0. National Institute of Standards and Technology, Standard Reference Data Program, Gaithersburg.
Neksa, P., Dorin, F., Rekstad, H., Bredesen, A., 2001. Measurements and experience on semi-hermetic CO2 compressors. In: Proc. 4th International Conference on Compressors and Coolants. IIR, Slovak Republic.
Petrenko, V.O., 1978. Investigation of ejector cooling machine operating with refrigerant R142b. Odessa Technological Institute of Refrigeration Industry: Ukraine, Ph.D. thesis.
Petrenko, V.O., 2001. Principle of working fluid selection for ejector refrigerating systems. Refrig. Eng. Technol. 1 (70), 16–21.
Petrenko, V.O., Chumak, I.G., Volovyk, O.S., 2005a. Comparative analysis of the performance characteristics of an ejector refrigerating machine utilizing various low-boiling working fluids. Refrig. Eng. Technol. 5 (97), 25–35.
Petrenko, V.O., Volovyk, O.S., Ierin, V.O., 2005b. Areas of effective application of ejector refrigerating machines using low-boiling refrigerants. Refrig. Eng. Technol. 1 (93), 17–30.
Robinson, D.M., Groll, E.A., 1998. Efficiencies of transcritical CO_2 cycles with and without an expansion turbine. Int. J. Refrigeration 21 (7), 577–589.